Development and applications of hypoplastic constitutive models

A dissertation submitted for habilitation

David Mašín

December 2009

Charles University in Prague
Institute of Hydrogeology, Engineering Geology and Applied Geophysics

Contents

Chapter 1

Introduction

This thesis is a summary of the research by the author and coworkers on hypoplastic constitutive models, undertaken in the period between years 2004 and 2009. By the time the research started, hypoplasticity was used mainly for predicting the behaviour of granular materials, such as sands or gravels. The most notable model is the one by von Wolfferdorff [47], which may be seen as a basic outcome of the research work carried out at the University in Karlsruhe during 80's and 90's. In addition to the models for granular soils, several modifications to predict the behaviour of fine grained soils were available [11, 33] and theoretical aspects of hypoplasticity were understood into a great detail (see Niemunis [34] for a summary). The author of this thesis proposed a conceptually simple hypoplastic model for clays that was aimed to be easy to use in practical applications. In subsequent research, the predictive capabilities of the model were extended to a number of different special materials. The model was implemented into a number of finite element codes and applied for solving practical problems.

This Habilitation thesis is subdivided into two main parts. The first is an overview part, in which the research is briefly outlined in the form of short summarising chapters. The overview part of the thesis is followed by an Appendix part, with fulltexts of selected key publications. Not all papers discussed in the overview part are present in the Appendix part, however. The overview part of the Habilitation thesis is subdivided into three main chapters. Chapter 2 describes the basic hypoplastic model for clays and its evaluation with respect to experimental data. Chapter 3 presents modifications of the model to predict the behaviour of different special materials. Finally, several examples of the use of the model in practical applications are described in Chapter 4.

The research described in the thesis was carried out by the author himself [21, 22, 24, 25, 23], in cooperation with his colleagues and coworkers [28, 9, 31, 29, 30, 8] and, importantly, by the MSc and PhD students supervised or co-supervised by the author [10, 45, 32, 42, 43]. Especially the research effort by the PhD the students from our research group at Charles University, namely V. Hájek [10], J. Najser [32], T. Svoboda [42, 43], R. Suchomel [40] and J. Trhlíková [45] is greatly appreciated. The research would not have started and continued without help and support by Dr. Jan Boháč and Prof. Ivo Herle.

Chapter 2

Basic hypoplastic model for clays and its evaluation

2.1 A hypoplastic model for clays [21]

Development of a new constitutive model is described step-by-step in Reference [21]. First, shortcomings of the hypoplastic model for soils with low friction angles by Herle and Kolymbas [11] are outlined. It is then proposed to improve this model by taking into account "generalised hypoplasticity" principles by Niemunis [34]. The general rate formulation of the proposed model reads

$$\overset{\circ}{\mathbf{T}} = f_s \boldsymbol{\mathcal{L}} : \mathbf{D} + f_s f_d \mathbf{N} \|\mathbf{D}\| \tag{2.1}$$

where $\overset{\circ}{\mathbf{T}}$ is an objective stress rate, $\mathbf{D}$ is the Euler's stretching tensor, $\boldsymbol{\mathcal{L}}$ and $\mathbf{N}$ are fourth- and second-order constitutive tensors, f_s and f_d are so-called barotropy and pyknotropy factors respectively. The tensor $\mathbf{N}$ is calculated by

$$\mathbf{N} = \boldsymbol{\mathcal{L}} : \left(-Y \frac{\mathbf{m}}{\|\mathbf{m}\|} \right) \tag{2.2}$$

Degree of nonlinearity Y and the tensor $\mathbf{m}$ may be seen as hypoplastic equivalents of a yield surface and a flow rule. The particular components of the model (namely Y, $\mathbf{m}$, f_s, f_d and $\boldsymbol{\mathcal{L}}$) are derived in such a way that the model has the following properties:

1. Y is chosen such that the limit state locus in the stress space (defined by $\overset{\circ}{\mathbf{T}} = \mathbf{0}$) corresponds with the formulation by Matsuoka-Nakai [20], with critical state friction angle φ_c as a model parameter.

2. $\mathbf{m}$ implies that the critical state is predicted – for $\overset{\circ}{\mathbf{T}} = \mathbf{0}$ at the critical state void ratio the model predicts zero volumetric strains ($\operatorname{tr} \mathbf{D} = 0$).

3. f_s is chosen such that for the given value of f_d the model is positively homogeneous of degree 1 in $\mathbf{T}$, i.e. soil behaviour may be normalised by the mean stress p. Consequently, normal compression lines are linear in the $\ln p$ vs. $\ln(1 + e)$ plane. The

isotropic normal compression line is defined by

$$\ln(1+e) = N - \lambda^* \ln \frac{p}{p_r} \tag{2.3}$$

with the reference stress $p_r = 1$ kPa and parameters N and λ^* that control its position and slope, respectively.

4. The pyknotropy factor f_d controls the influence of overconsolidation ratio. It is defined in the way ensuring that the critical state line in the $\ln p$ vs. $\ln(1+e)$ space reads

$$\ln(1+e) = N - \lambda^* \ln 2 - \lambda^* \ln \frac{p}{p_r} \tag{2.4}$$

and the slope of the isotropic unloading line from the isotropic normally consolidated state is in the $\ln p$ vs. $\ln(1+e)$ plane defined by the parameter κ^*.

5. The hypoelastic tensor $\boldsymbol{\mathcal{L}}$ implies that the shear stiffness is controlled by the last model parameter, r. It also ensures that a correct initial shear stiffness is predicted when the model is used together with the intergranular strain concept [36].

In summary, the model requires five constitutive parameters, namely φ_c, N, λ^*, κ^* and r. These parameters correspond to the parameters of the Modified Cam clay model and, in principle, only two experiments are required for their calibration – an isotropic loading and unloading test for N, λ^* and κ^* and a triaxial shear test for φ_c and r.

The model is evaluated with respect to experimental data on London clay. It is demonstrated that although the proposed model requires smaller number of parameters than the reference model, its predictions are more accurate. More detailed evaluation of predictive capabilities of the model is given in Section 2.4.

2.2 State boundary surface [28]

A natural component of many elasto-plastic models is so-called state boundary surface, a hypersurface in the stress vs. void ratio space that bounds all admissible states. This surface, experimentally well confirmed, is not incorporated explicitly in hypoplastic models. The prediction of this surface by the proposed model has been studied in ref. [28].

Thanks to the fact that for the given f_d the proposed model is positively homogeneous of degree 1 in $\mathbf{T}$, its behaviour may be normalised by the Hvorslev equivalent pressure at the isotropic normal compression line p_e^* defined by

$$p_e^* = p_r \exp\left[\frac{N - \ln(1+e)}{\lambda^*}\right] \tag{2.5}$$

Taking into account Eq. (2.5), rate of the normalised stress $\mathbf{T}_n = \mathbf{T}/p_e^*$ is given by

$$\dot{\mathbf{T}}_n = \frac{f_s}{p_e^*}\left(\boldsymbol{\mathcal{L}} : \mathbf{D} + f_d \mathbf{N} \|\mathbf{D}\|\right) + \frac{\mathbf{T}\,\mathrm{tr}\,\mathbf{D}}{p_e^* \lambda^*} \tag{2.6}$$

Limit surface in the stress vs. void ratio space, named *swept-out-memory* (SOM) surface, defined by $\dot{\mathbf{T}}_n = \mathbf{0}$, may be found by solving Eq. (2.6) for unknowns $\mathbf{D}$ and f_d. As the model is positively homogeneous of degree 1 in $\mathbf{D}$ (i.e., rate independent), $\|\mathbf{D}\|$ may take an arbitrary positive value, for simplicity $\|\mathbf{D}\| = 1$. It was shown that at the swept-out-memory surface the pyknotropy factor f_d reads

$$f_d = \|f_s \boldsymbol{\mathcal{A}}^{-1} : \mathbf{N}\|^{-1} \tag{2.7}$$

with the corresponding direction of stretching

$$\vec{\mathbf{D}} = -\frac{\boldsymbol{\mathcal{A}}^{-1} : \mathbf{N}}{\|\boldsymbol{\mathcal{A}}^{-1} : \mathbf{N}\|} \tag{2.8}$$

where the fourth-order tensor $\boldsymbol{\mathcal{A}}$ reads

$$\boldsymbol{\mathcal{A}} = f_s \boldsymbol{\mathcal{L}} + \frac{1}{\lambda^*} \mathbf{T} \otimes \mathbf{1} \tag{2.9}$$

Eqs. (2.7-2.9) allow us to plot the shape of the SOM surface. For reasonable values of the material parameters (namely, as discussed in [28], for $\kappa^* < \lambda^*/4$), its shape is close to the experimentally confirmed shape predicted by the Modified Cam clay model, as demonstrated in Fig. 2.1. Unlike the Cam clay model, however, the hypoplastoc SOM surface correctly excludes tensile stresses.

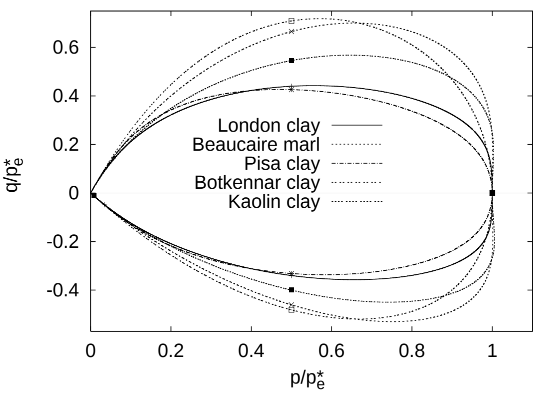

Figure 2.1: SOM surface of the hypoplastic model for clays for five different sets of material parameters (London clay [21]; Beaucaire marl [31]; Kaolin [10]; Bothkennar and Pisa clay [22]).

Last, the difference between the SOM surface and the state boundary surface is studied in [28]. By means of normalised response envelopes and an analytical derivation of the tangent to the SOM surface it is shown that the state boundary surface does not coincide with the SOM surface. However, taking into account the uncertainties in the experimental determination of the state boundary surface, for most applications they may be assumed as coinciding.

2.3 Graphical representation of the model [9]

Many theories, based on different mathematical approaches, emerged from the research on soil constitutive modelling. Even though the models may be developed to be easy to use, with low number of parameters and well-defined calibration procedures, their mathematical formulations are often rather complex and only few scientists, working on their development, understand it into detail. For this reason, Gudehus and Mašín [9] developed a way for graphical representation of constitutive equations, which eases judgment of predictive capabilities of the models. Using the proposed representation the authors have demonstrated that the elasto-plastic models based on the critical state soil mechanics and the clay hypoplastic model, though being fundamentally different algebraically, have the same physical grounds.

Gudehus and Mašín [9] focused on representation of tangential stiffness using concept of so-called response envelopes [7] and on representation of state limits – states approached asymptotically by monotonous deformations with constant direction of the strain rate tensor.

The response envelopes are polar diagrams for unit strain rates plotted in the plane $\dot{\sigma}'_1$ vs. $\sqrt{2}\dot{\sigma}'_2$ (see Fig. 2.2).

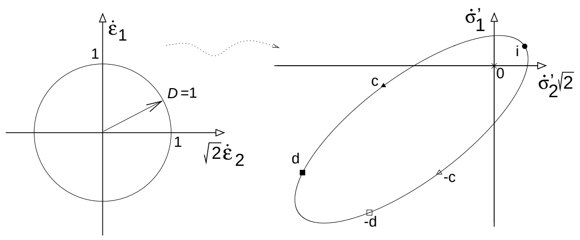

Figure 2.2: Response envelope of stress rates due to unit strain rates [9].

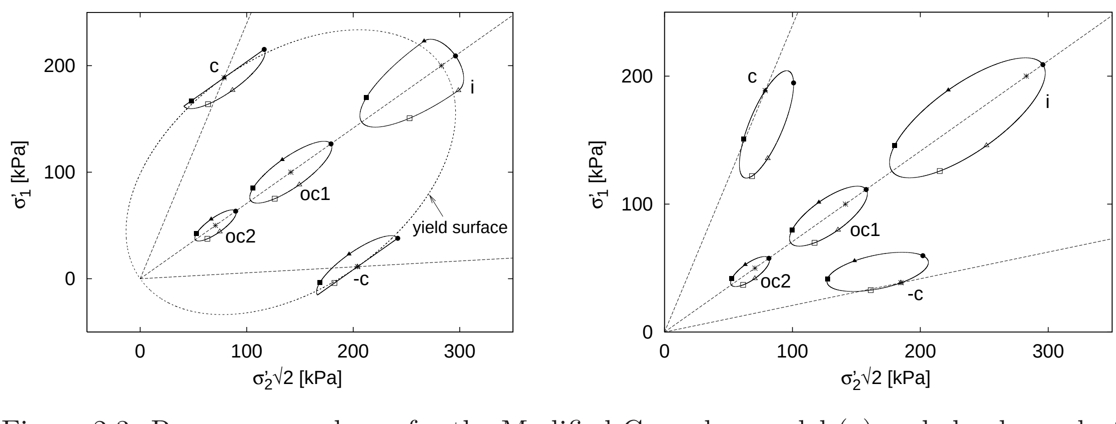

Figure 2.3: Response envelopes for the Modified Cam clay model (a) and clay hypoplastic model (b) [9].

The response envelopes for different special stress states are plotted in Fig. 2.3a for the Modified Cam clay model and in Fig. 2.3b for the hypoplastic model. The envelopes have different shapes – the elasto-plastic envelopes consist of two elliptical sections centered about the reference state, one corresponding to elasto-plastic loading and the second to elastic unloading. Hypoplastic response envelope is elliptic and translated with respect to the reference state. However, there are clear similarities between the responses by the elasto-plastic and hypoplastic models, such as isochoric (constant volume) response for the stress state corresponding to the critical state, higher stiffness in isotropic unloading then in loading, etc.

Comparison of the graphical representation of state limits, also presented in [9], further demonstrated that not only these special states (isotropic state, critical state), but all state limits in general are predicted similarly by the elasto-plastic and hypoplastic models. This fact is important, as state limits represent a fundamental feature of soil behaviour that should be captured by the models. Advantage of hypoplastic models thus does not lie in different predictions of the state limits, these are predicted reasonably well also by existing elasto-plastic models, but in capturing the non-linear character of soil response.

2.4 Evaluation of predictive capabilities of the model

2.4.1 Directional response [31]

The parameters of the proposed constitutive model may be found using a relatively limited number of laboratory experiments with given stress paths (isotropic loading and unloading and drained triaxial shear test). However, stress paths experienced by the soil in the real boundary value problem have a very general nature, pointing in different directions in the stress space. A good constitutive model should be capable of representing the soil behaviour under such general conditions.

A comprehensive experimental program that focused on the directional response of a reconstituted fine-grained soil may be found in [2]. These data were used by Mašín et al. [31] for the evaluation of the proposed model. For reference, the proposed model has been compared with different advanced constitutive models, both elasto-plastic and hypoplastic, namely the three surface kinematic hardening (3-SKH) model [39], Grenoble-type hypoplastic model (CLoE) [1] and the Modified Cam clay model [38]. In order to reproduce the situation often occurring in geotechnical design, the constitutive models have been calibrated using experimental data on isotropically consolidated samples and their predictive capabilities were then checked with respect to the data on anisotropically consolidated soil (response envelopes are shown in Fig. 2.4).

The clay hypoplastic model enhanced by the intergranular strain concept and the 3-SKH model performed the best. As expected, the basic version of the hypoplastic model (without the intergranular strain concept) underestimated small strain stiffness for stress probes that followed after a sharp stress path reversal. This was (to a much bigger extent) true also for the basic Modified Cam clay model. The CLoE model performed the worst. This

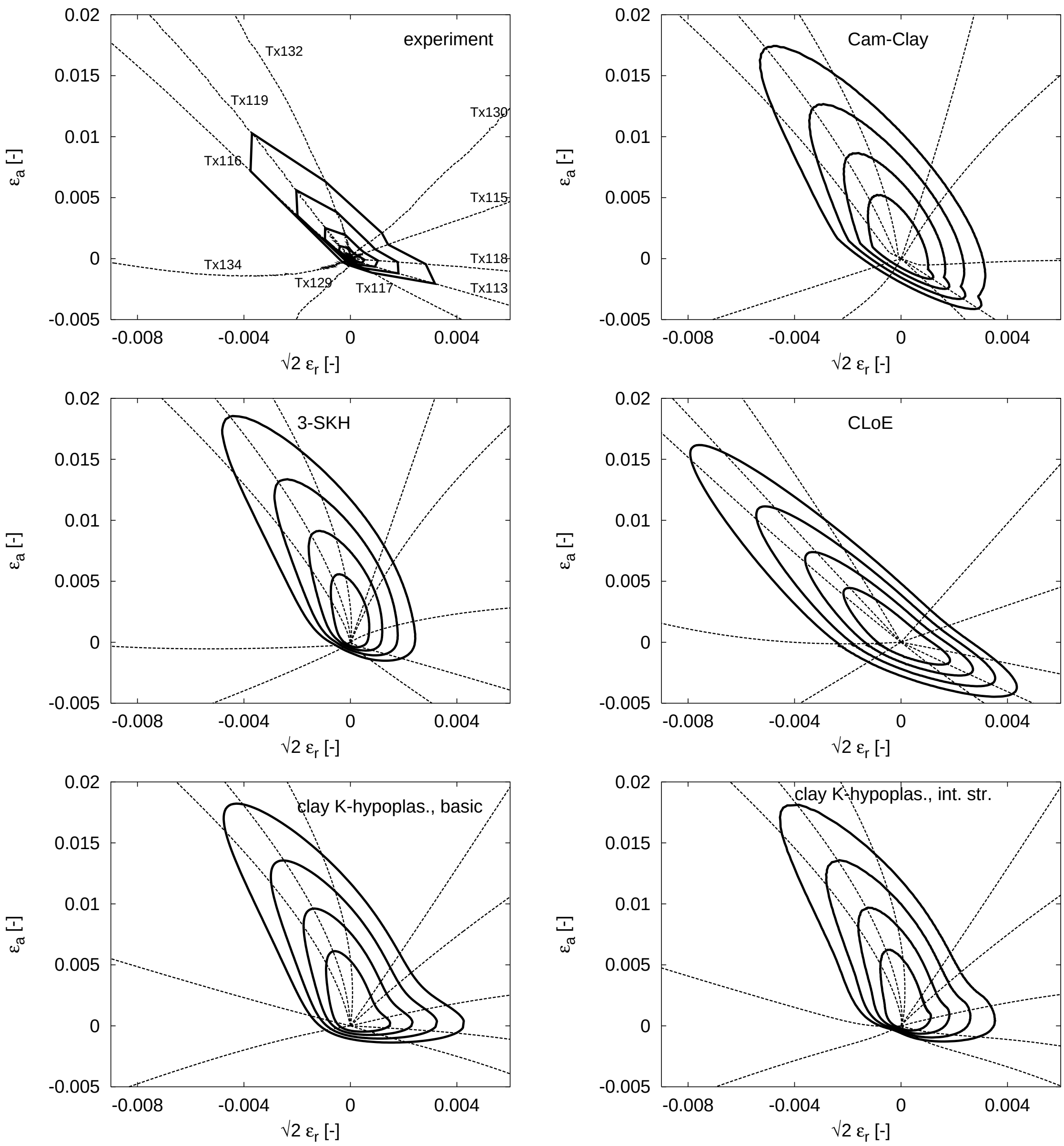

Figure 2.4: Experimental *vs.* simulated strain response envelopes for $R_\sigma = 20$, 30, 40 and 50 kPa [31].

is a consequence of the fact that this model has not been developed specifically for the prediction of behaviour of fine-grained soils and it belongs to the class of hypoplastic models referred to as *amorphous*, i.e., it does not consider void ratio as a state variable.

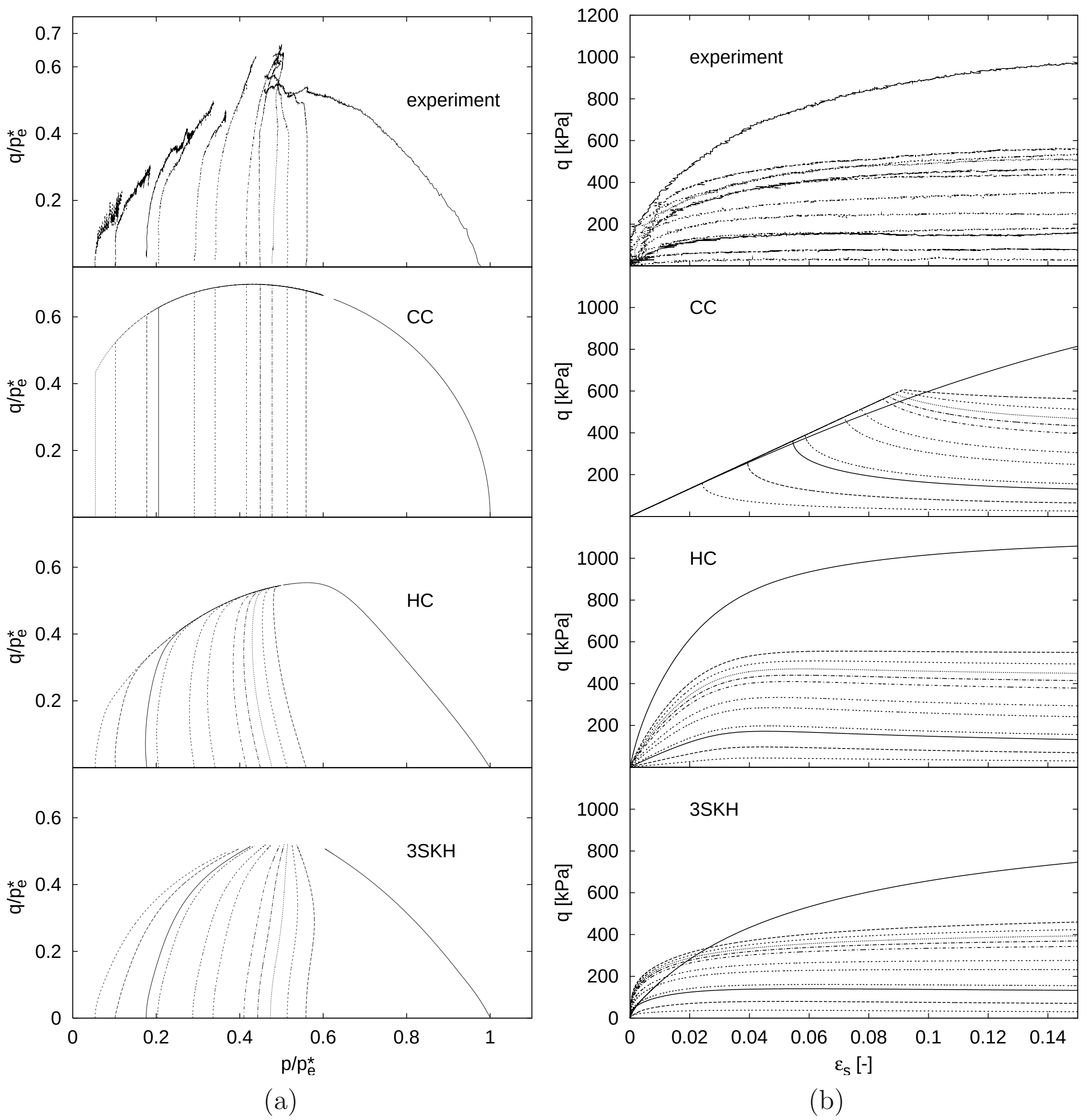

Figure 2.5: Stress paths normalised by p_e^* (a) and q vs. ϵ_s graphs (b) for $OCR = 10$ optimised parameters [10].

2.4.2 The influence of overconsolidation ratio [10]

It has been recognized since the development of critical state soil mechanics in 1960's that realistic constitutive models should consider void ratio e as a state variable. This approach, in theory, allows us to use a single set of material parameters to predict the behaviour of soils with a broad range of overconsolidation ratios (OCR) and thus simplifies application of constitutive models in practice. As a matter of fact, however, qualitatively correct predictions of the behaviour of soils with different $OCRs$ based on a single set of material parameters do not necessarily imply satisfactory performance from the quantitative point of view. An evaluation of the hypoplastic model with respect to different experimental data give Hájek et al. [10]. Predictions by the hypoplastic model have been compared with different elasto-plastic models, namely the 3-SKH model and the Modified Cam clay (CC) model. The evaluation revealed that:

1. For higher $OCRs$ the hypoplastic model (HC) performs less correctly than other two models when calibrated using data for $OCR = 1$. However, when calibrated at higher OCR, it produces the best predictions of all tested models for the entire range of $OCRs$, with more-or-less constant value of an error measure err.

2. The elasto-plastic (CC and 3SKH) models calibrated at $OCR = 10$ perform relatively correctly up to $OCR \approx 4$. For lower $OCRs$ parameters for normally consolidated state lead to better predictions, but in the case of 3SKH still worst than predictions by hypoplasticity.

3. Further, the predictions of failure states have been studied by plotting the peak friction angles φ_p with respect to OCR. The hypoplastic model and the 3-SKH model compared well with the experimental data, while the Modified Cam clay model overpredicted φ_p significantly.

For illustration, stress-strain diagrams by the different constitutive models are shown in Fig. 2.5.

2.5 Improvement for undrained conditions [29]

As pointed out by Niemunis [34] and by Huang et al. [13], shortcoming of hypoplastic models in general is an incorrect prediction of the initial portion of the undrained stress path, particularly for tests on normally consolidated soils at the isotropic stress states. A conceptually simple modification of the basic hypoplastic model, which overcomes this drawback, has been proposed by Mašín and Herle [29]. The modified model is applicable to both normally consolidated and overconsolidated soils and predicts the same swept-out-memory states (i.e., normal compression lines) as the original model. At anisotropic stress states and at higher overconsolidation ratios the modified model yields predictions similar to the original model.

The modified model takes the form

$$\overset{\circ}{\mathbf{T}} = f_s \left(\boldsymbol{\mathcal{L}}^D : \mathbf{D} + w_y f_d \mathbf{N} \|\mathbf{D}\| \right) \tag{2.10}$$

in which the weight factor w_y is equal to 0 at the isotropic stress state, $w_y = 1$ for $\varphi_{mob} \geq \varphi_c$, and a suitable interpolation function is chosen for the states in between. The tensor $\boldsymbol{\mathcal{L}}^D$ is at the isotropic stress state bi-linear in $\mathbf{D}$. Because at the isotropic stress state $w_y = 0$, Eq.

(2.10) is at the isotropic state equivalent to an elasto-plastic model with response envelope composed of two elliptic sections centered about the reference stress state (Fig. 2.6). The direction of the initial portion of the undrained stress path is thus perpendicular to the p-axis (Fig. 2.7), which better agrees with the experimental data.

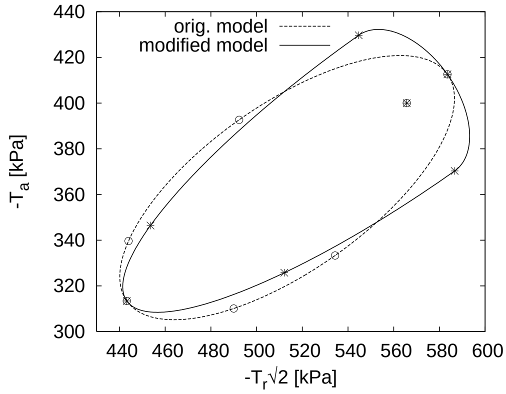

Figure 2.6: Response envelopes at the isotropic normally compressed stress state predicted by the original and modified models [29].

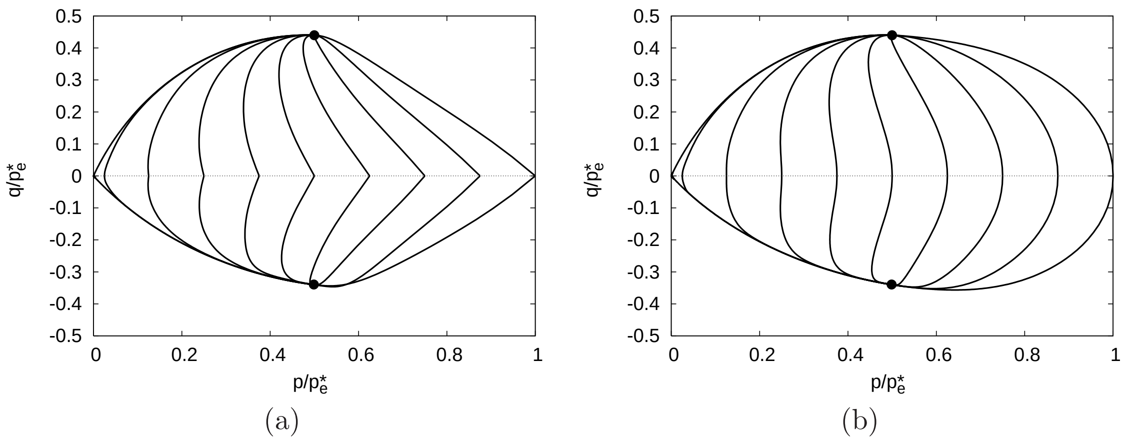

Figure 2.7: Stress paths of undrained compression and extension tests with different initial values of $OCRs$. The original model (a) and the modified model (b) [29].

A suitable interpolation function for $\boldsymbol{\mathcal{L}}^D$ for non-isotropic states is chosen to ensure that the basic hypoplastic model is recovered for $w_y = 1$ (i.e. for $\varphi_{mob} \geq \varphi_c$) and for all swept-out-memory states.

Though the modification of the model is conceptually valuable as it overcomes one of the model limitations, it is pointed out that for practical applications the basic model may be used. Predictions by the basic and modified models do not differ significantly for K_0 normally consolidated and overconsolidated soils, which are states present in the ground.

Chapter 3

Modifications of the model to predict the behaviour of nonstandard materials

3.1 Model for structured/cemented clays

3.1.1 Basic model for structured clays [22]

The basic hypoplastic model for clays has been modified in order to include the effects of structure in natural clays [22]. The difference in the behaviour of natural and reconstituted clays is caused by different particle arrangement (fabric) and inter-particle bonding. A conceptual framework for the incorporation of structure into constitutive models has been proposed by Cotecchia and Chandler [3]. For most applications a single scalar state variable, so-called sensitivity s, is sufficient to represent the effects of structure in natural soils. The sensitivity is a measure of ratio of sizes of state boundary surfaces of natural and reference (reconstituted) materials.

Thanks to the availability of the analytical formulation of the state boundary surface (Sec. 2.2), the incorporation of structure into the proposed hypoplastic model is relatively straightforward. It may be shown that the size of the state boundary surface is increased s-times if the Hvorslev equivalent pressure p_e^* is multiplied by s in the expression for the pyknotropy factor f_d.

In order to model progressive changes of structure caused by the degradation of inter-particle bonding, a suitable evolution equation for sensitivity must be defined. A possible choice reads

$$\dot{s} = -\frac{k}{\lambda^*}(s - s_f)\dot{\epsilon}^d \tag{3.1}$$

where k and s_f are model parameters controlling the rate of structure degradation and the final sensitivity and $\dot{\epsilon}^d$ is a rate of a damage strain, defined as

$$\dot{\epsilon}^d = \sqrt{(\dot{\epsilon}_v)^2 + \frac{A}{1-A}(\dot{\epsilon}_s)^2} \tag{3.2}$$

where $\dot{\epsilon}_v$ and $\dot{\epsilon}_s$ are rates of total volumetric and shear strains respectively and A is a model parameter. A few other changes into the basic hypoplastic model must be included in order to ensure consistency between model predictions and pre-defined structure degradation law (3.1) and in order to preserve physical meaning of the parameters κ^* and r.

The influence of the new model parameters A, k and s_f is demonstrated by means of normalised incremental strain response envelopes, see Fig. 3.1. The parameter k controls the overall rate of structure degradation, whereas the parameter A controls the influence of the shear strain component, keeping the volumetric response unchanged.

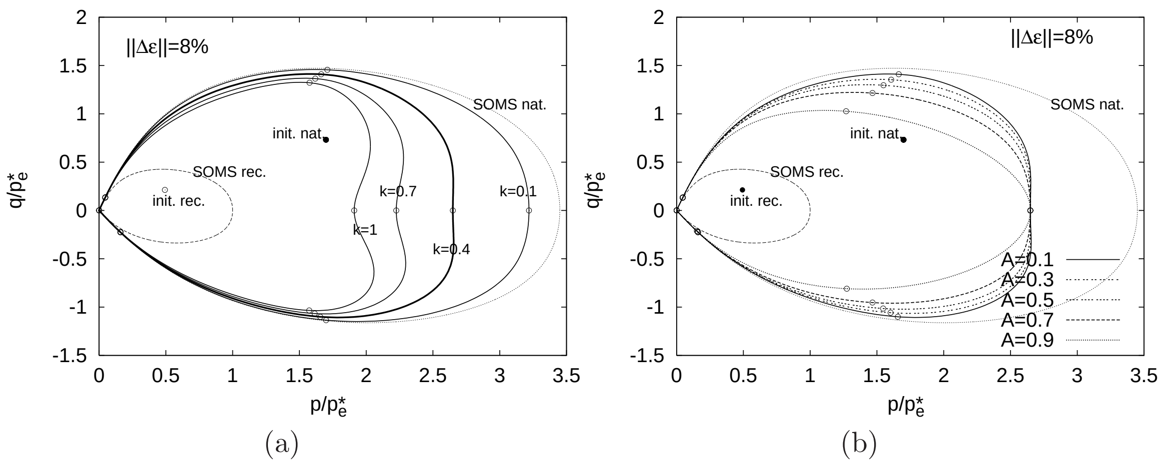

Figure 3.1: The influence of the parameter k (a) and A (b) on the shape and size of the incremental strain response envelopes for the given value of $\|\Delta\varepsilon\|$ [22].

3.1.2 Evaluation of the model for structured clays [24]

Mašín [24] compared predictions of the model for structured clays with predictions by different elasto-plastic models by means of experimental data on natural and reconstituted Pisa and Bothkennar clays. First, an elasto-plastic "equivalent" (from the point of view of required material parameters), structured Modified Cam clay model (SMCC), has been developed. In addition, the hypoplastic response was compared with response by advanced elasto-plastic models based on kinematic hardening plasticity.

Figure 3.2 shows predictions of normalised stress paths (a) and volumetric response (b) for the hypoplastic and SMCC models. Advantage of the non-linear hypoplastic formulation is revealed. The hypoplastic model predicts a gradual structure degradation process that takes place also inside the state boundary surface and becomes more intensive as the state moves towards this surface. It was further shown that the advanced kinematic hardening elasto-plastic models give predictions of similar accuracy as the hypoplastic model.

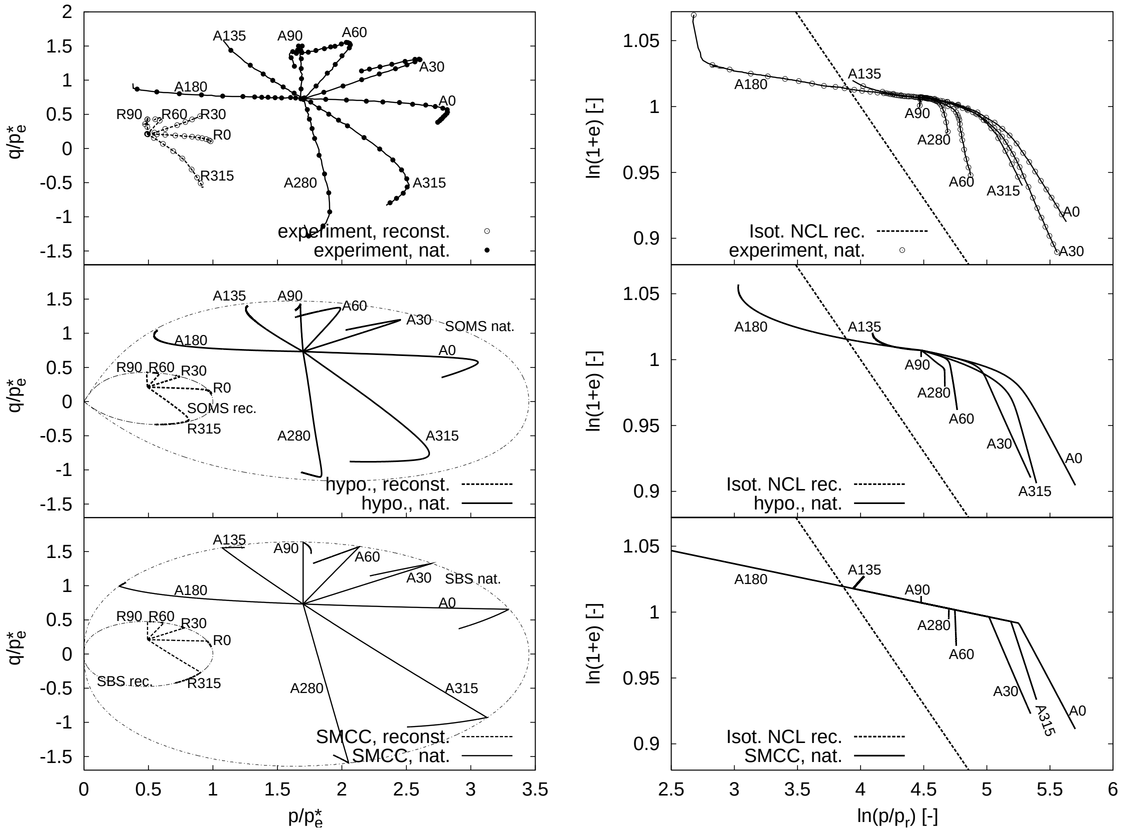

(a) (b)

Figure 3.2: (a) Normalised stress paths of the natural and reconstituted Pisa clay and (b) experiments on natural Pisa clay in the volumetric plane. Experimental data and predictions by the structured hypoplastic model and SMCC model [24].

3.1.3 Model for the small-strain shear stiffness behaviour [45]

In order to predict the soil behaviour in the very-small strain range, the model for structured clays must be combined with the intergranular strain concept [36]. The concept may be applied directly as proposed in Ref. [36], without any modification. As discussed by Mašín [21], the model formulation implies that

$$G_0 = \frac{m_R}{r\lambda^*} p \tag{3.3}$$

The very small strain shear modulus G_0 is thus linearly dependent on the mean stress, and additional state variables void ratio e and sensitivity s do not influence the value of G_0.

The dependency of G_0 on the cementation structure has been studied by Trhlíková et al. [45] using tests on artificially cemented Kaolin clay. It was confirmed that the very small strain shear modulus depends on overconsolidation ratio (OCR), as proposed by Viggiani and Atkinson [46]. In addition, G_0 has been found to be strongly dependent on the amount of cementation, measured by sensitivity s (Fig. 3.3).

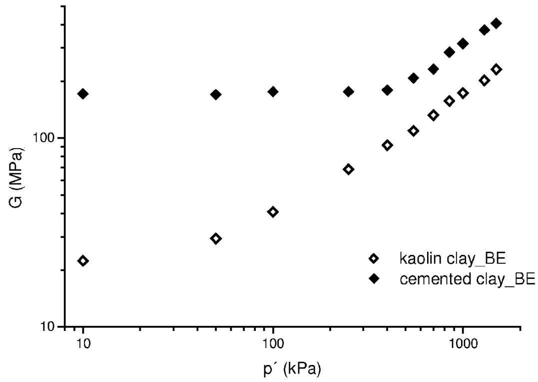

Figure 3.3: The dependency of G_0 on mean stress for reconstituted and cemented Kaolin clay [45].

Based on these experimental data and several other data sets taken over from the literature, Trhlíková et al. [45] proposed the following equation for the dependency of G_0 on OCR and s:

$$\frac{G_0}{p_r} = A_G \left(\frac{p}{p_r}\right)^n \left(\frac{s}{s_f}\right)^l OCR^m \tag{3.4}$$

where p_r is a reference stress 1 kPa, $OCR = p_e^*/p$ is the isotropic overconsolidation ratio with p_e^* being the Hvorslev equivalent pressure, A_G is a model parameter and s_f is the final sensitivity (see Sec. 3.1.1). The Eq. (3.4) is graphically represented in Fig. 3.4.

Incorporation of Eq. (3.4) into the hypoplastic model for cemented soils from Sec. 3.1.1 is relatively straightforward. In the new model, the intergranular strain model parameter m_R is no-more considered as constant, but it is a variable dependent on the state variables. Comparison of Eqns. (3.3) and (3.4) leads to

$$m_R = r\lambda^* A_G \left(\frac{p}{p_r}\right)^{(n-1)} \left(\frac{s}{s_f}\right)^l OCR^m \tag{3.5}$$

The enhanced model predicts G_0 by Eq. (3.4), while the other properties of the basic model for cemented materials remain unchanged.

In the past, different authors reported different dependencies of G_0 of cemented soils on the mean stress. Some authors observed a decrease of G_0 at the threshold mean stress at which the cementation bonds start to break, other authors reported gradual increase of G_0 with p. One of the interesting consequences of the model formulation is shown in Fig. 3.5.

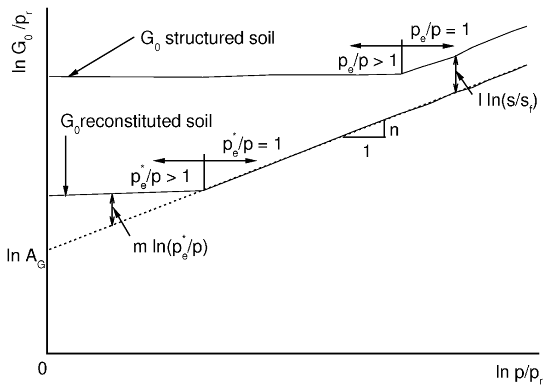

Figure 3.4: Graphical representation of Eq. (3.4) [45].

In Fig. 3.5b, the dependency of G_0 on p predicted by the enhanced hypoplastic model for cemented soils is plotted for different values of the parameter k (i.e. for different rates of structure degradation). The corresponding compression lines are in Fig. 3.5a. Using the enhanced model, it may be shown that the drop or gradual increase of G_0 with p at the structure degradation threshold depend on the rate of structure degradation measured by the parameter k. The observations by different authors can thus be explained within a unified framework, which is based on Eq. (3.4).

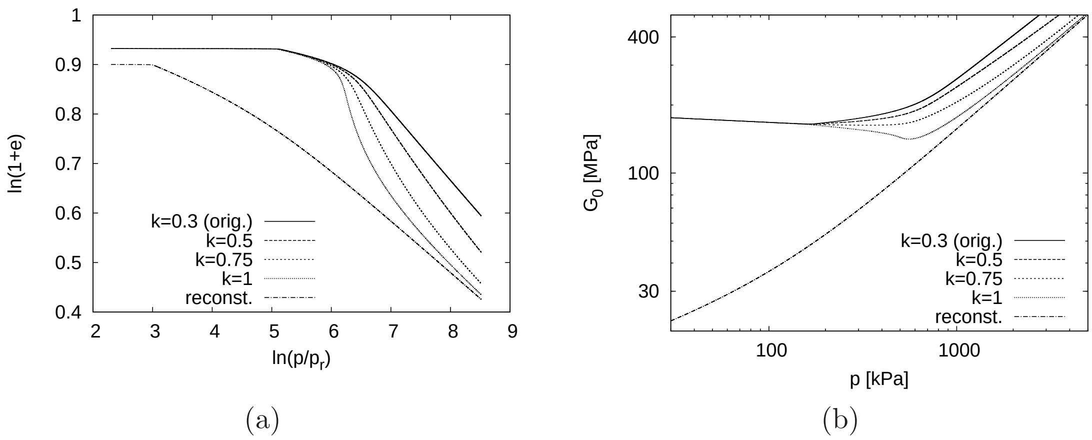

Figure 3.5: Compression lines for different values of the parameter k (a) and predictions of G_0 by the enhanced hypoplastic model for cemented soils (b) [45].

3.2 Model for unsaturated soils

3.2.1 Hypoplastic model for the mechanical response of unsaturated soils [30]

The basic hypoplastic model is applicable to predicting the behaviour of saturated soils. One of the important modifications of the model extends its applicability to simulating the mechanical behaviour of unsaturated materials. The hypoplastic model for unsaturated soils was proposed by Mašín and Khalili [30].

Central to the new model is description of the stress state within an unsaturated soil. It now becomes generally accepted that two stress variables are needed for proper description of the stress state within unsaturated soil. A tensorial stress measure describing the averaged action of external forces and fluid pressures on the soil skeleton and a scalar stress measure quantifying the stiffening effect of water menisci on the skeleton.

The tensorial stress measure $\mathbf{T}$ may be in general written as

$$\mathbf{T} = \mathbf{T}_{tot} - \chi u_w \mathbf{1} - (1-\chi) u_a \mathbf{1} = \mathbf{T}_{net} - \chi s \mathbf{1} \tag{3.6}$$

where $\mathbf{T}_{tot}$ is a total stress, u_a is the pore air pressure and u_w is the pore water pressure, $\mathbf{T}_{net}$ is the net stress defined as $\mathbf{T}_{net} = \mathbf{T}_{tot} - u_a\mathbf{1}$ and s is matric suction $s = -(u_a - u_w)$. χ is the Bishop factor.

Different formulations for the factor χ are adopted by different researchers. In one of the possible approaches, the tensorial variable is selected in such a way that it forms a frame within which the unsaturated soil behaviour can be uniquely described. Such a tensorial stress measure can then be seen as an equivalent to the effective stress in saturated materials. The additional scalar stress variable is needed to control the size of the state boundary surface. Suitability of different stress measures was studied by Khalili et al. in [17, 15]. They proposed the following formulation for the factor χ:

$$\chi = \begin{cases} 1 & \text{for} \quad s < s_e \\ \left(\dfrac{s_e}{s}\right)^{\gamma} & \text{for} \quad s \geq s_e \end{cases} \tag{3.7}$$

where s_e is the air entry value of suction (or air expulsion for wetting processes) and γ is an empirical coefficient. It was shown that the best-fit value of the exponent $\gamma = 0.55$ is suitable to represent the behaviour of different soil types.

The following modifications have been introduced into the reference hypoplastic model for saturated materials in order to predict the behaviour of unsaturated soils:

- The effective stress tensor for saturated soils $\mathbf{T}$ has been replaced by the effective stress formulation for unsaturated soils by Khalili et al. [17, 15] (Eqns. (3.6) and (3.7)).
- The additional scalar stress state variable (suction s) controls the size of the state boundary surface. Thus, the parameters N and λ^* of the basic model are not soil

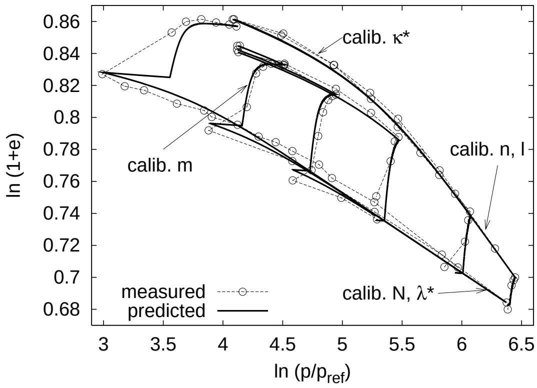

Figure 3.6: Isotropic compression tests at constant suction and wetting tests at constant net stress by Sun et al. [41] replotted in the effective stress space with superimposed predictions by the proposed model [30].

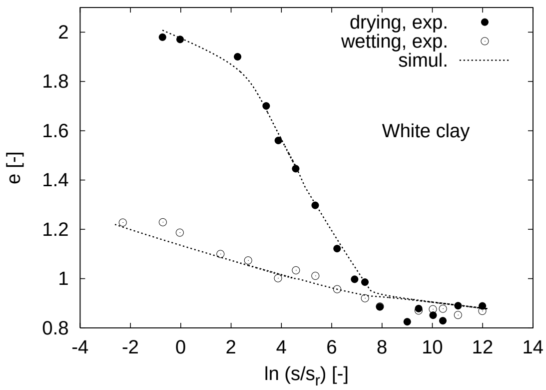

Figure 3.7: Drying-wetting test on White clay. Experimental data by Fleureau et al. [5] compared with simulations by the proposed hypoplastic model [30].

parameters in the new model, but rather they are variables that depend on the value of s. Obviously, the model formulation ensures that the limit values of N and λ^* for saturated soils are obtained for $s = 0$.

- Loose soils (soils with low OCRs) are known to experience so-called wetting induced collapse. The collapse is manifested by a decrease in void ratio associated with suction decrease, and it occurs even at constant effective stress. In order to predict this phenomenon, the basic formulation of the hypoplastic model was enhanced by the tensorial variable $\mathbf{H}$ and a new pyknotropy factor f_u in the following way:

$$\overset{\circ}{\mathbf{T}} = f_s \left(\boldsymbol{\mathcal{L}} : \mathbf{D} + f_d \mathbf{N} \|\mathbf{D}\| \right) + f_u \mathbf{H} \tag{3.8}$$

The variable $\mathbf{H}$, which allows us to predict straining $\mathbf{D}$ even at $\overset{\circ}{\mathbf{T}} = \mathbf{0}$, is active only for suction decrease at low $OCRs$ and it is derived to ensure consistency at the state boundary surface (calculated using method described in Sec. 2.2).

The new model was evaluated using experimental data on different soils that included wetting (suction decrease) experiments, drying (suction increase) response and constant-suction tests at different suction levels. For illustration, Figure 3.6 shows response to isotropic compression tests at constant suction and wetting tests at constant net stress by Sun et al. [41]. Fig. 3.7 shows results of drying-wetting test on White clay by Fleureau et al. [5] compared with predictions by the proposed model.

3.2.2 Model for the hydraulic response [25]

In order to perform coupled hydro-mechanical analyses of geotechnical problems in unsaturated soils, the mechanical model for unsaturated soils must be combined with suitable hydraulic model describing the water retention curve (WRC), i.e. the dependency of a degree of saturation of S_r on suction s. The hypoplastic model from Sec. 3.2.1 can be, in principle, combined with a number of existing hydraulic models for unsaturated soils. As shown by Mašín [25], however, the choice of this model cannot be completely arbitrary, as different models may lead to inconsistencies when used with the effective stress equation (3.7) with constant s_e. To overcome these limitations, a new model for WRC was developed by Mašín [25]. Among other features, this model quantifies the dependency of s_e, appearing in the effective stress equation of the mechanical model, on void ratio. The model thus couples the hydraulic and mechanical responses of unsaturated soils.

The model is based on the effective stress principle for unsaturated soils described in Sec. 3.2.1. Based on several fundamental assumptions, one of which is an assumption of the existence of generalised elastic and plastic potentials defined in terms of effective stress for unsaturated soils, Khalili et al. [19, 16] derived the following expression for the rate of S_r with the rate of s and e:

$$\dot{S}_r = \frac{\partial S_r}{\partial s}\dot{s} + \frac{\psi - S_r}{e}\dot{e} \tag{3.9}$$

The first term quantifies the dependency of S_r on suction at constant void ratio (WRC), and the second term evaluates the dependency of S_r on void ratio at constant suction. The factor ψ from Eq. (3.9) can be calculated from χ (Eq. (3.7)) using $\psi = d(\chi s)/ds$.

Eq. (3.9), together with the known value of the factor ψ, can be used to evaluate variation of S_r with e at constant suction. An assumption of uniqueness of the main wetting and drying branches of WRCs in the S_r vs. s vs. e space then allows us to derive an expression for the dependency of WRC on void ratio. The derivation always starts from the predefined WRC for the reference void ratio e_0. An example of such a "water retention state surface" (WRSS) is shown in Fig. 3.8. As a part of the new model, the dependency of s_e on e is defined. This dependency is then used as an enhancement of the hypoplastic model for unsaturated soils.

The new model does not require *any* material parameters, apart from parameters specifying WRC for the reference void ratio e_0. This is an advantage when compared with many

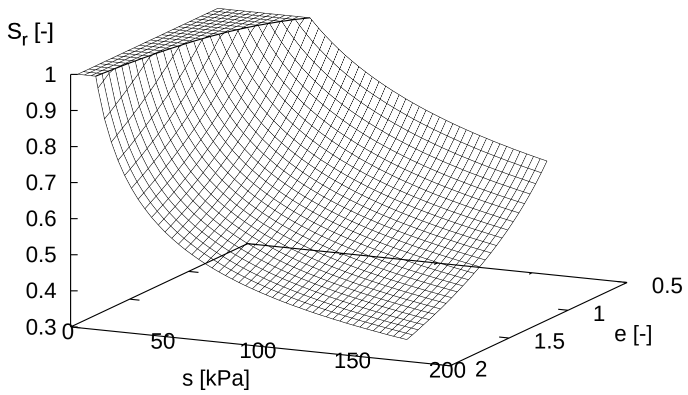

Figure 3.8: Predicted state surface in the s vs. e vs. S_r space [25].

existing models for WRCs, in which the dependency of WRC on e is typically controlled by empirical formulations requiring additional model parameters.

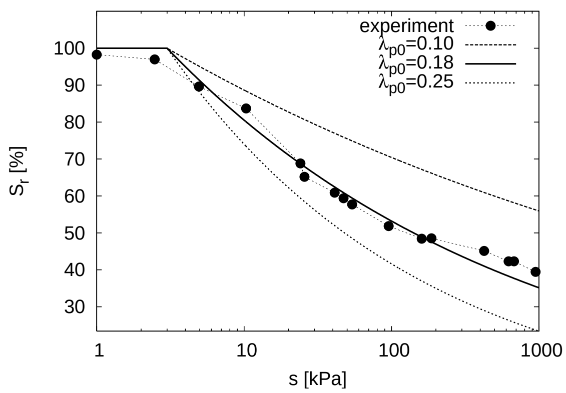

Figure 3.9: Wetting branch of WRC of HPF type quartz silt used for calibration of the proposed model [25], experimental data from [14].

An example evaluation of the new model with respect to experimental data on HPF quartz silt by Jotisankasa et. al [14] is given in Figs. 3.9 and 3.10. Figure 3.9 shows a water retention curve used for calibration of all model parameters. The parameters were calibrated using WRC at a reference void ratio e_0 (changes of e during measurement of WRC were neglected). These parameters were then used to calculate S_r in tests in which the variation of e is significant, namely suction-monitored oedometric tests at constant water content. Good agreement between the measured and predicted responses (Fig. 3.10) demonstrates predictive capabilities of the proposed model.

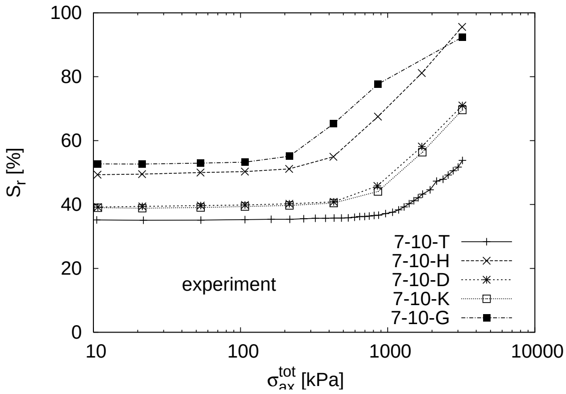

(a)

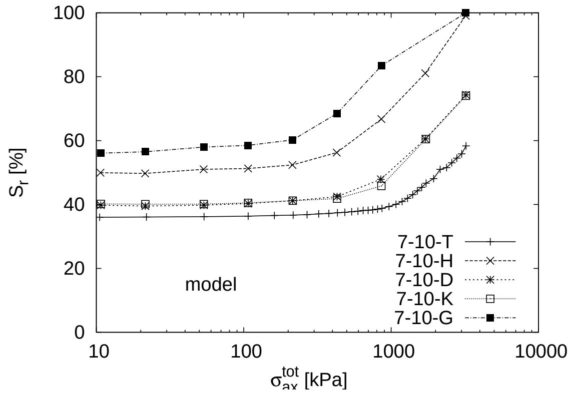

(b)

Figure 3.10: Results of suction-monitored oedometric tests at constant water content from [14] (a), compared with model predictions (b) [25].

3.3 Model for double porosity materials [32]

Another special type of soils with unusual mechanical behaviour are lumpy clays. These clays, which for example form landfills of some open cast coal mines, are examples of the so-called double porosity materials. These materials are characteristic by two distinct pore systems. In addition to the voids within intact clay lump (intragranular porosity) the lumpy soil has also voids between the clay lumps (intergranular porosity). Lumpy clays deserve attention of geotechnical engineers, as they cover large areas with potential for engineering development.

The behaviour of the double porosity material is characteristic by high compressibility. With increasing load, the double porosity structure degrades and the intergranular voids close up. Ultimately, at high stresses, all intergranular voids close up and the overall mechanical behaviour of the soil resembles the behaviour of the reference lump material.

An approach to predict the behaviour of such a material has been proposed by Mašín et al. [26] and Koliji et al. [18]. It is summarised in Najser et al. [32]. It is based on the similarity between the behaviour of the lumpy soil and soil with meta-stable structure due to cementation. The approach is demonstrated in Fig. 3.11. The reference model is used to predict the behaviour of clayey lumps, which have intragranular porosity only. In the model, the additional intergranular porosity due to double porosity structure is allowed for by increasing the size of the state boundary surface. The intergranular porosity and the double porosity structure degrades during straining of the material, similarly to the degradation of cementation structure in soft natural clays.

The approach was applied by Najser et al. [32] to predict the behaviour of lumpy soil using the hypoplastic model for structured clays from Sec. 3.1.1. The model was evaluated

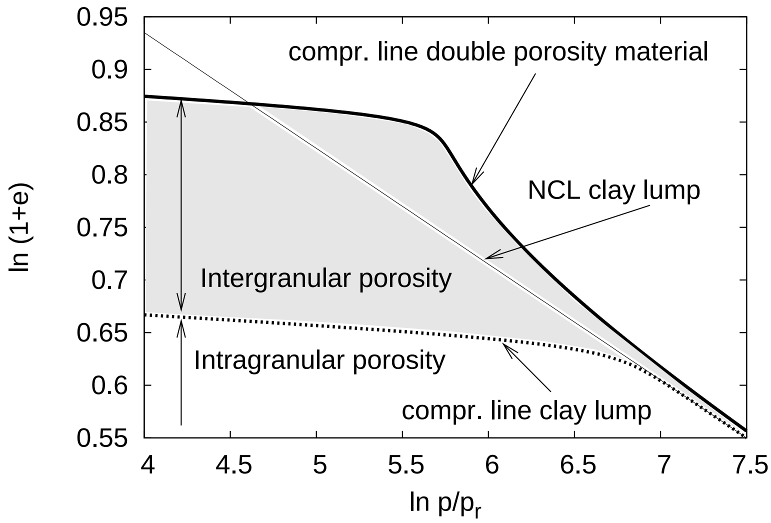

Figure 3.11: Modelling the behaviour of clays with double-porosity structure [32].

with respect to experimental data on laboratory specimens with scaled-down granulometric curves, geotechnical centrifuge models and real-size trial motorway embankments. More details on this application of the model are given in Sec. 4.5.

Chapter 4

Clay hypoplasticity in practical applications

4.1 Finite element implementation and the soilmodels.info project [8]

Most of the finite element codes currently used in geotechnical practice allow to implement different constitutive models via user-defined subroutines. As practicing engineers generally have neither the time nor the expertise to implement the models into finite element codes by themselves, their choice of models remains confined to the few (often primitive) models that happen to be already available in commercial FE codes. Thus, current situation in geotechnical engineering is such that the research on soil behaviour and constitutive modelling is well in advance of every-day practice. In order to promote the use of advanced models in practice, robust implementation of the models must be available to practitioners.

For this reason, a freely available database of constitutive models has been set up by a group of internationally recognised experts in the field. The database is available at the *www.soilmodels.info* web site. Setup of the database was announced to the geotechnical engineering community through an open letter to the editor published in the International Journal for Numerical and Analytical Methods in Geomechanics [8]. The site was accessed 2808 times in the period between September 2007 and November 2009.

The soilmodels.info site contains several implementations of the clay hypoplastic model. The model is available for all finite element codes supporting *umat* format of ABAQUS and for the PLAXIS finite element code through an interface implementation. Fig. 4.1 shows a map of the World with countries from which the hypoplastic model implementation was downloaded indicated in blue colour. In addition to the soilmodels.info implementation, the hypoplastic model was implemented directly into the commercial finite element package Tochnog Professional.

Several examples of practical applications of the hypoplastic model are presented in the

Figure 4.1: Map of the World showing downloads of clay hypoplastic implementation from www.soilmodels.info.

following sections. In these examples, advantages originating from the use of advanced constitutive models, instead of the most popular simple models, are emphasized.

4.2 Heathrow express trial tunnel [23]

Heathrow express trial tunnel [4], a NATM tunnel built in London Clay to test effectiveness of the shotcrete lining method, has since become a classical example for evaluation of different numerical tools. This tunnel was modelled by Mašín [23] using 3D finite element analysis. Different constitutive models were calibrated using high quality experimental data on London Clay by Gasparre [6]. Figure 4.2 shows stiffness degradation curves in the small and very-small strain range, compared with predictions by the hypoplastic model.

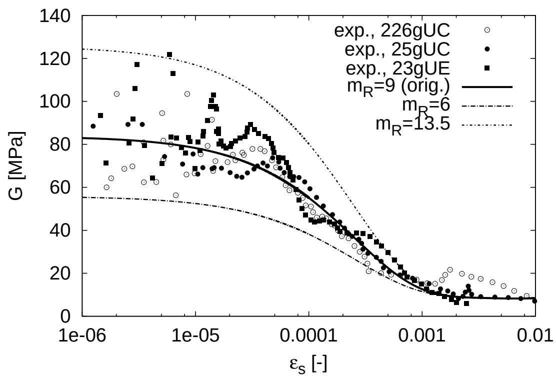

Figure 4.2: Stiffness degradation curves simulated by the hypoplastic model with different parameters [23]. Experimental data on natural samples of London Clay from [6].

All the simulations were performed with constitute models calibrated solely on the basis of laboratory experiments, without tuning material parameters to obtain monitored deformations. High K_0 values varying with depth, as measured in situ in [12], were considered. Shotcrete lining was represented by a linear elastic model with time-dependent stiffness. Finite element mesh and the modelled geometry are shown in Fig. 4.3.

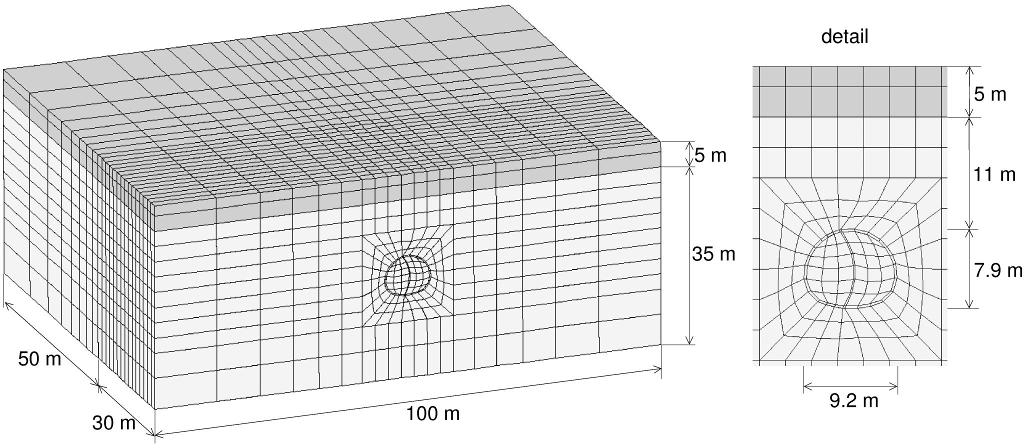

Figure 4.3: Finite element mesh used in the analyses of the Heathrow express trial tunnel [23].

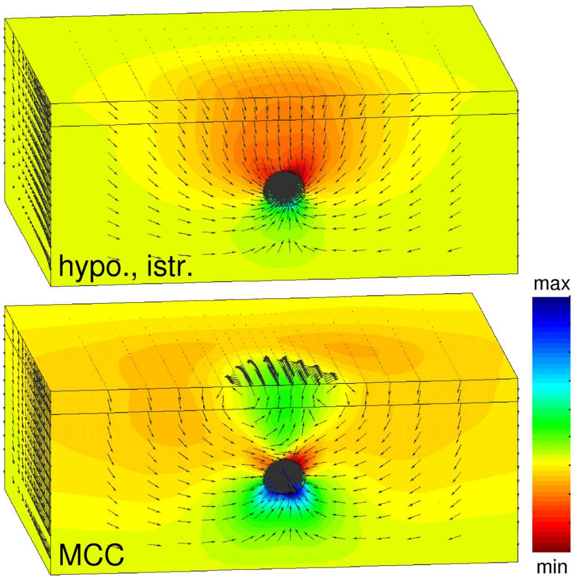

Figure 4.4: Predictions of the Heathrow express tunnel by different constitutive models. Contour lines show vertical displacements, vectors show displacement direction [23].

The overall displacement fields at the end of the tunnel excavation predicted by the hypoplastic model with intergranular strain concept (hypo.,istr.) and the Modified Cam clay model (MCC) are shown in Fig. 4.4. The figure shows that the MCC model predicts an upward heave of the soil wedge above the tunnel. Such a heave, which is caused by the high K_0 value of London clay and which is obviously unrealistic, is not predicted by the non-linear hypoplastic model.

A surface settlement trough and measurements of an inclinometer located in a distance of 7 m from the tunnel are shown in Fig. 4.5. Predictions by the hypoplastic model are in a reasonable agreement with the measurement, although it slightly overestimates the settlement trough width and magnitude of horizontal displacements. Predictions by the Modified Cam clay model are unrealistic.

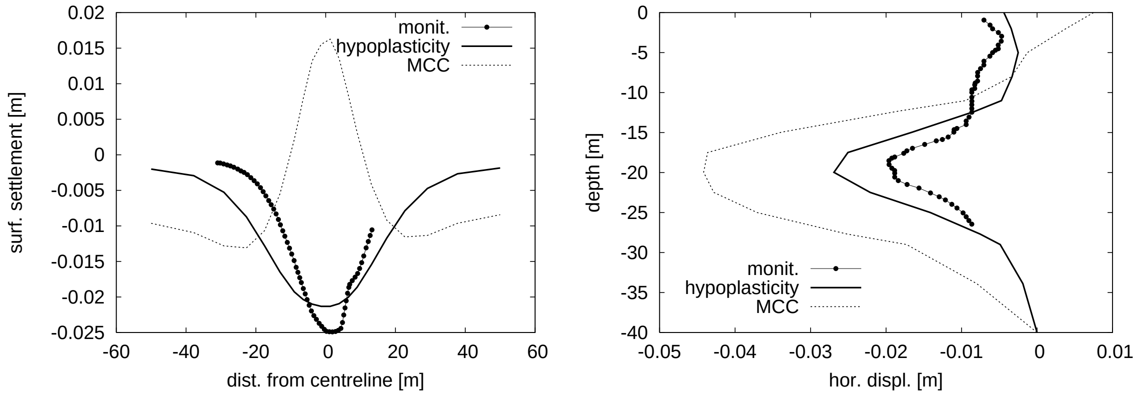

(a) (b)

Figure 4.5: The influence of soil constitutive model on numerical predictions (monitoring data from [4]).

In addition to comparison of predictive capabilities of different constitutive models, Mašín [23] studied the influence of different material parameters on the calculated results. It was shown that both the large-strain and small-strain stiffness soil characteristics have pronounced influence on the calculated results. The rate of increase of the shotcrete lining stiffness also influence the calculated results significantly.

4.3 Dobrovského tunnel and exploratory adits [42]

The second case study analysed is an exploratory adit of the Dobrovskeho tunnel, which is being excavated in Brno, Czech Republic. The tunnels consist of two oval tunnel tubes with lengths 1.2 km, height of about 12 m and a section width of about 14 m. Both the tunnels are led parallel at a distance of 70 m and are being excavated by the NATM with vertical face sequence subdivided into 6 segments. The overburden ranges between 6 and 21 m. For exploration purposes, three adits were excavated. The exploratory adits had approximately triangular cross sections with side length 5 m and they were situated in the tunnel top headings (Fig. 4.6). The subsoil in which the tunnels are excavated consists of Miocene limy, silty stiff clay (Brno Clay). The natural cover of the Brno Clay deposits is represented by Quaternary loess loams, clayey loams and sandy gravel.

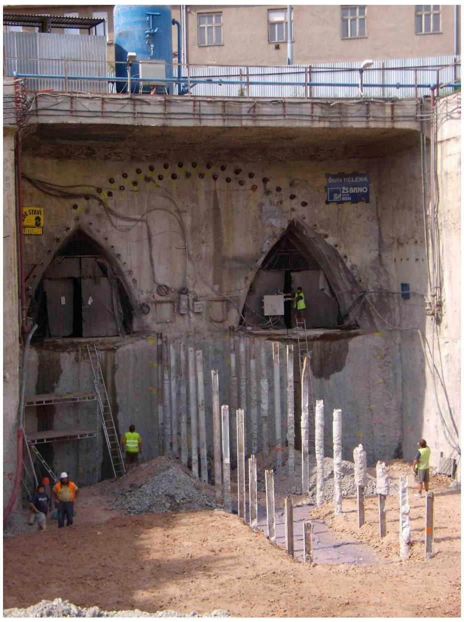

Figure 4.6: Exploratory adits situated in the top heading of the future Dobrovskeho tunnel.

Full 3D numerical model of the exploratory adit has been developed by Svoboda and Mašín [42]. The 3D analyses of the whole tunnel are presented in [43]. The parameters of the hypoplastic and Mohr-Coulomb models were calibrated on the basis of quality laboratory experiments that included measurements of small strain stiffness characteristics using local LVDT strain transducers and bender elements. As no measurements of the coefficient of earth pressure at rest K_0 have been performed on the site, simulations were performed with two different values of K_0, namely $K_0 = 1.25$ and $K_0 = 0.66$.

The approach to the simulations was as follows:

- First, two selected constitutive models (hypoplastic model for clays and Mohr-Coulomb model) were calibrated using experimental data on Brno clay. This parameter set was used for 3D simulations of exploratory adit.
- Results of simulations were compared with monitoring data. The hypoplastic model gave predictions in a reasonable agreement with monitoring, whereas the Mohr-Coulomb model significantly overestimated the displacements. The monitoring data were then used to optimise the constitutive model parameters. For this purpose, UCODE optimisation software [37] was used. The optimisation was based on plane strain analyses using convergence-confinement method (CCM). Adequacy of the CCM representation of the 3D effects was first checked (Sec. 4.4). During optimisation, only minor change of the hypoplastic parameters was necessary to obtain accurate fit of the measured surface settlement trough. The Mohr-Coulomb model could be successfully optimised for low value of K_0 only and the required change of the parameter E was substantial. The predictions with original and optimised parameter

sets are in Fig. 4.7.

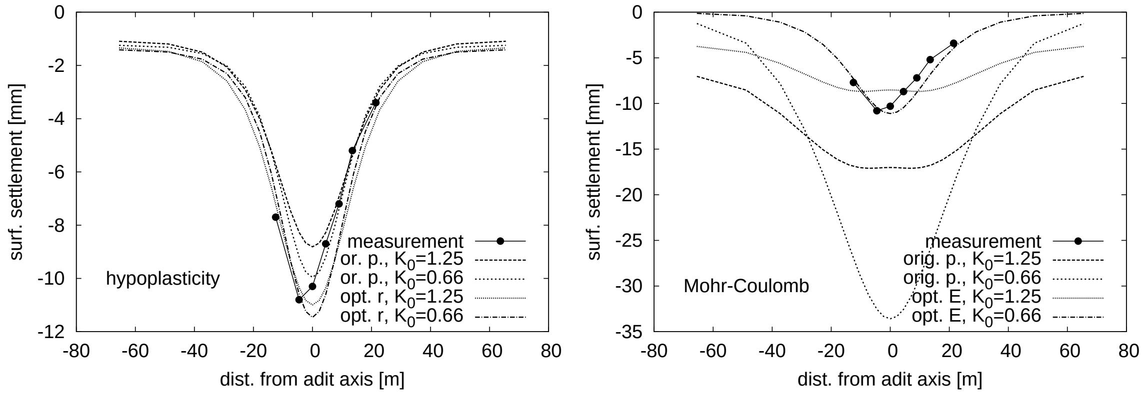

(a) (b)

Figure 4.7: Surface settlement troughs due to the Dobrovskeho exploratory adit calculated with original and optimised parameter sets by the hypoplastic model (a) and Mohr-Coulomb model (b) [44].

- The optimised parameters were used in 3D simulations of the whole Dobrovskeho tunnel using the hypoplastic model. Finite element model that realistically reproduces the complex excavation sequence was developed for this purpose (Fig. 4.8a). The results, shown in Fig. 4.8b, represent class A predictions, as the tunnel has not been built by the time the model was developed. The predicted surface settlement trough is in Fig. 4.8b compared with monitoring data obtained in several profiles close to the simulated cross-section. The simulated results agree well with the observations.

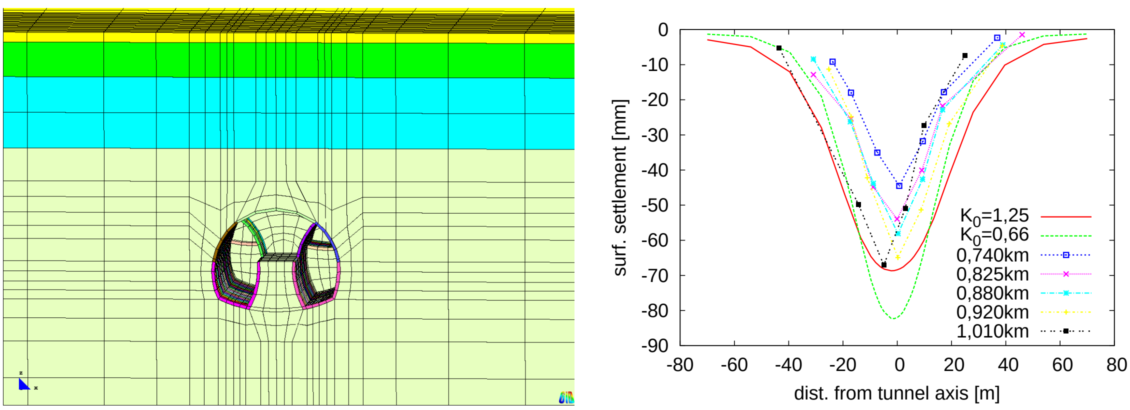

(a) (b)

Figure 4.8: 3D model of the Dobrovskeho tunnel (a) and surface settlement troughs predicted for two different K_0 values (b).

4.4 Evaluation of the convergence-confinement method for modelling NATM tunnels using plane-strain analysis [43]

Simplified procedures that allow us to consider 3D effects within a simplified 2D plane strain analysis are still popular in geotechnical design. One of the reasons may be the fact that set up of the full 3D model is inevitably, regardless the computer power, time consuming process and it might not be feasible at preliminary design stages or for less demanding tunneling problems. The second, perhaps surprising reason, stands in the fact that the available research studies are not conclusive in demonstration that the predictive capabilities of full 3D methods are higher than those of properly used 2D analyses with indirect incorporation of 3D effects. Unfortunately, evaluation of the 2D methods by means of comparison with fully 3D simulations is not common in the technical literature dealing with numerical simulations of tunneling problems. For this reason, Svoboda and Mašín [43] evaluated the most common 2D method for simulation of NATM tunnels, so-called convergence-confinement (or stress release) method (CCM), with respect to the 3D analyses presented in Sections 4.2 and 4.3. In all cases, simulations by the hypoplastic model were used.

The CCM method requires specification of a single parameter denoted as λ^d, quantifying stress reduction along the tunnel boundary at the time of lining installation. Fictitious pressure σ_r^f at the tunnel boundary at the time of lining installation can thus be calculated from the initial stress in the ground σ_r^0 from

$$\sigma_r^f = (1 - \lambda^d)\sigma_r^0 \tag{4.1}$$

Svoboda and Mašín [43] optimised the value of λ^d using an optimisation software UCODE to ensure the 2D and 3D methods predict as closely as possible the surface settlement trough. The overall displacement field was studied subsequently.

The following observations were made:

- λ^d depends on the assumed material parameters, i.e. on the soil type. The very small strain shear modulus G_0 influences λ^d remarkably. Interestingly, λ^d does not appear to be influenced significantly by the large strain shear modulus G_{ls}. This result might appear surprising, as both G_0 and G_{ls} were shown to have substantial effect on the predicted displacements. One of the consequences of this observation is that a change of geological conditions during excavation of a single tunnel might require appropriate modification of λ^d values used in the simulations.
- K_0 does not appear to have substantial effect on λ^d.
- For the same soil type, the tunnel size and geometry influences significantly appropriate values of λ^d. In the case of the Dobrovskeho study, $\lambda^d \approx 0.5$ was found for the exploratory adit, whereas $\lambda^d \approx 0.3$ for the whole tunnel. Thus, if λ^d found on the basis of results of an exploratory adit simulations was used for predictions of the full tunnel response, it would lead to an overestimation of the tunnel deformations.

The vertical displacement fields by the 2D and 3D methods are compared in Figure 4.9. The surface settlement troughs by the 2D and 3D methods match very well. An overall agreement could have been expected, as λ^d was calibrated with the intention to match the surface settlement trough as accurately as possible, but it is interesting to observe that also the settlement trough shape is predicted accurately by the 2D method. Variation of vertical and horizontal displacements with depth show good agreement for the Heathrow express case. For both Dobrovskeho adit and Dobrovskeho tunnel, the 2D method does not give the same answers as the 3D method within a distance of approximately 1 tunnel diameter from the tunnel. The predictions match well outside this region.

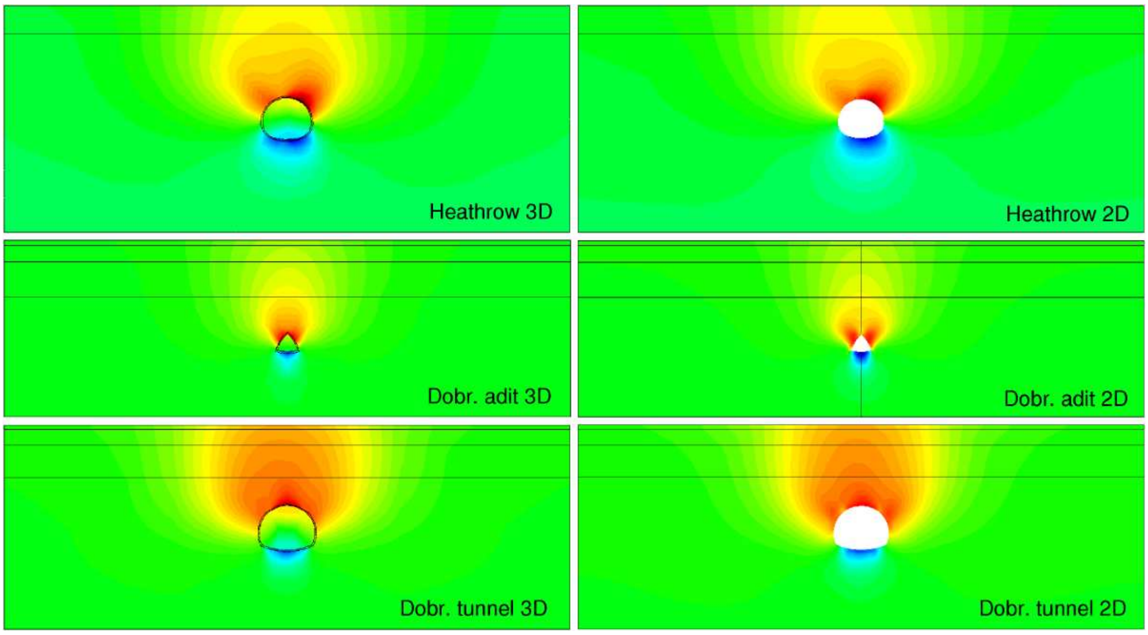

Figure 4.9: Qualitative comparison of vertical displacement fields predicted by the 3D and 2D methods for the three case studies analysed (the same color scale for corresponding 2D and 3D analyses) [43].

4.5 Modelling motorway embankments on double porosity soils [32]

An approach to model double-porosity lumpy soil, summarised in [32], was presented in Sec. 3.3. Najser et al. [32] further evaluated the model by means of simulations of motorway embankments on colliery landfills composed of lumpy clay material. The embankments were 6 and 7.5 m high respectively, they were constructed on a landfill of 30 m thickness and monitored for 3 and 5 years respectively.

The hypoplastic model was first calibrated using experimental data. Parameters of the basic model were calibrated using experiments on reconstituted soil (which were shown to represent also the behaviour of the material of the lump). Parameters describing the effects of double-porosity structure were then calibrated using oedometric experiments on lumpy material with scaled-down granulometry (Fig. 4.10)

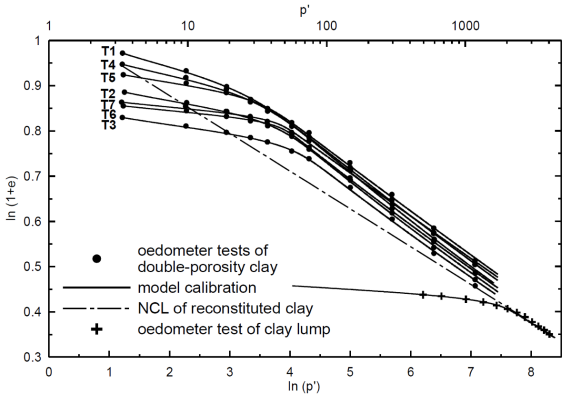

Figure 4.10: Calibration of the structure degradation related parameters using oedometric specimens on material with scaled-down granulometry [32].

The second step was evaluation of the hypoplastic model by means of simulations of centrifuge tests of embankments on double-porosity soils with scaled-down granulometry. The centrifuge tests were performed at ETH, Zurich. Good agreement between the measured and predicted settlements of the embankment demonstrated predictive capabilities of the model.

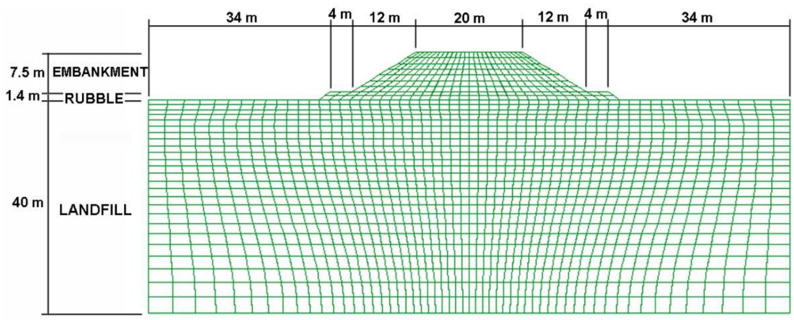

Figure 4.11: Geometry and finite element mesh of numerical model of the embankment 2 [32].

Finally, the trial motorway embankments were simulated using coupled consolidation analyses. Figure 4.11 shows finite element mesh of an embankment 2. The results of numerical modelling showed significantly higher settlements below the embankments than measured in situ. This is shown in Fig. 4.12, which depicts distributions of vertical displacements with depth. The differences between the predicted and observed results were attributed to the degradation of the double porosity structure due to weathering during 20 years after the landfill construction. The degradation was subsequently incorporated into the numerical model by reducing void ratio and sensitivity. The settlements by the updated model agreed well with the monitoring data (Fig. 4.12). The amount of weathering destructuration needed to obtain the monitored settlements for the two models is shown in Fig. 4.13.

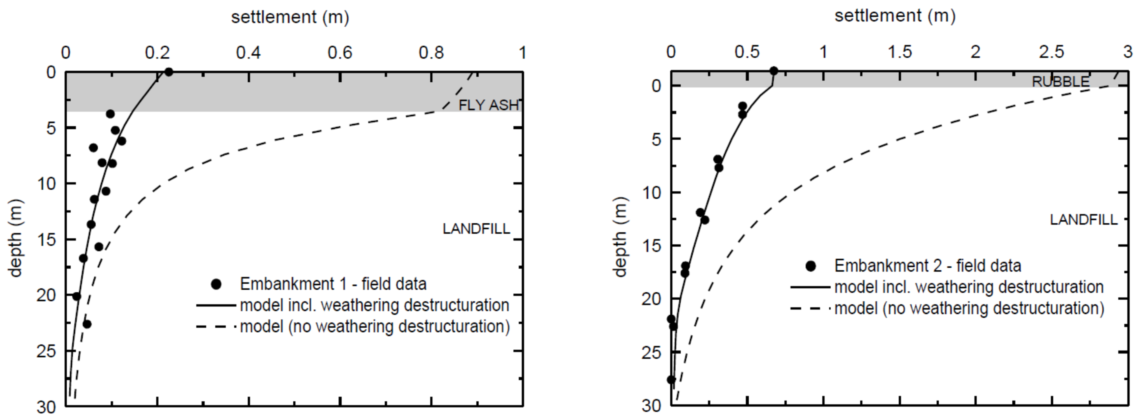

Figure 4.12: Distribution of vertical displacements with depth [32].

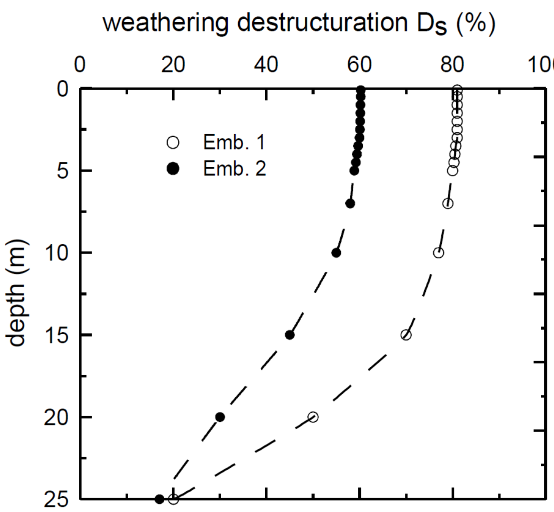

Figure 4.13: Degree of weathering destructuration needed to obtain the monitored settlements [32].

The hypoplastic model in this case helps to understand features of the mechanical behaviour of clayfill material. Their knowledge may be helpful for the future design of engineering structures in a similar environment.

Chapter 5

Summary and conclusions

Almost 20 years of research based at the University of Karlsruhe consolidated into a critical-state based hypoplastic model for granular soils by von Wolffersdorff [47]. By the time the author started the research on hypoplasticity, hypoplastic models were used primarily for predictions of the behaviour of granular materials, such as sands and gravels. There were two notable exceptions: model for soils with low friction angles by Herle and Kolymbas [11], which was used as a reference model during the development of the basic model for clays, and a visco-hypoplastic model by Niemunis [33]. This second model was, however, not hypoplastic in a strict sense, as for higher OCRs it produced purely hypoelastic response (this shortcoming was corrected recently by Niemunis et al. [35]).

The author extended the field of application of hypoplastic models by proposing a rate-independent model for clays [21] with only few parameters equivalent to the parameters of the well-known Modified Cam clay model. The model itself, when combined with the intergranular strain concept by Niemunis and Herle [36], is suitable for predictions of the behaviour of reconstituted clays and stiff clays with stable structure. In a number of comparative studies it was shown that the model gives predictions of similar accuracy as advanced critical state based kinematic hardening elasto-plastic models.

The next step in the research was derivation of an analytical formulation for the state boundary surface predicted by the model [27]. This allowed us to extend the predictive capabilities of the model to a number of different special materials, such as clays with meta-stable structure due to cementation [22], unsaturated soils [30] and double porosity soils [32].

The model was implemented into a number of finite element codes, either directly (Tochnog Professional), or through user defined interface implementation (ABAQUS, PLAXIS). The implementation is freely available through the soilmodels.info web site [8]. Nowadays the model is used in research and practical applications worldwide. Its merits when compared with the use of simpler constitutive models were demonstrated in a number of comparative studies, summarised in Chapter 4 of this overview part of the Habilitation thesis.

References

[1] R. Chambon, J. Desrues, W. Hammad, and R. Charlier. CLoE, a new rate–type constitutive model for geomaterials. theoretical basis and implementation. *International Journal for Numerical and Analytical Methods in Geomechanics*, 18:253–278, 1994.

[2] D. Costanzo, G. Viggiani, and C. Tamagnini. Directional response of a reconstituted fine grained soil. Part I: Experimental investigation. *International Journal for Numerical and Analytical Methods in Geomechanics*, 30(13):1283–1301, 2006.

[3] F. Cotecchia and J. Chandler. A general framework for the mechanical behaviour of clays. *Géotechnique*, 50(4):431–447, 2000.

[4] A. P. Deane and R. H. Basset. The Heathrow express trial tunnel. *Proc. Instn. Civil Engineers*, 113:144–156, 1995.

[5] J.-M. Fleureau, S. Kheirbek-Saoud, R. Soemitro, and S. Taibi. Behaviour of clayey soils on drying-wetting paths. *Canadian Geotechnical Journal*, 30(2):287–296, 1993.

[6] A. Gasparre. *Advanced laboratory characterisation of London Clay*. PhD thesis, University of London, Imperial College of Science, Technology and Medicine, 2005.

[7] G. Gudehus. A comparison of some constitutive laws for soils under radially symmetric loading and unloading. In *Proc.* 3^{rd} *Int. Conf. on Numerical Methods in Geomechanics*, pages 1309–1323. Aachen, 1979.

[8] G. Gudehus, A. Amorosi, A. Gens, I. Herle, D. Kolymbas, D. Mašín, D. Muir Wood, R. Nova, A. Niemunis, M. Pastor, C. Tamagnini, and G. Viggiani. The soilmodels.info project. *International Journal for Numerical and Analytical Methods in Geomechanics*, 32(12):1571–1572, 2008.

[9] G. Gudehus and D. Mašín. Graphical representation of constitutive equations. *Géotechnique*, 52(2):147–151, 2009.

[10] V. Hájek, D. Mašín, and J. Boháč. Capability of constitutive models to simulate soils with different ocr using a single set of parameters. *Computers and Geotechnics*, 36(4):655–664, 2009.

[11] I. Herle and D. Kolymbas. Hypoplasticity for soils with low friction angles. *Computers and Geotechnics*, 31(5):365–373, 2004.

[12] D. W. Hight, A. Gasparre, S. Nishimura, N. A. Minh, R. J. Jardine, and M. R. Coop. Characteristics of the london clay from the Terminal 5 site at Heathrow airport. *Géotechnique*, 57(1):3–18, 2007.

[13] W.-X. Huang, W. Wu, D.-A. Sun, and S. Sloan. A simple hypoplastic model for normally compressed clay. *Acta Geotechnica*, 1(1):15–27, 2006.

[14] A. Jotisankasa, A. Ridley, and M. Coop. Collapse behaviour of compacted silty clay in suction-monitored oedometer apparatus. *Journal of Geotechnical and Geoenvironmental Engineering ASCE*, 133(7):867–877, 2007.

[15] N. Khalili, F. Geiser, and G. E. Blight. Effective stress in unsaturated soils: review with new evidence. *International Journal of Geomechanics*, 4(2):115–126, 2004.

[16] N. Khalili, M. A. Habte, and S. Zrgarbashi. A fully coupled flow-deformation model for cyclic analysis of unsaturated soils including hydraulic and mechanical hystereses. *Computers and Geotechnics*, 35(6):872–889, 2008.

[17] N. Khalili and M. H. Khabbaz. A unique relationship for χ for the determination of the shear strength of unsaturated soils. *Géotechnique*, 48(2):1–7, 1998.

[18] A. Koliji, L. Vulliet, and L. Laloui. New basis for the constitutive modelling of aggregated soils. *Acta Geotechnica*, 3(1):61–69, 2008.

[19] B. Loret and N. Khalili. A three-phase model for unsaturated soils. *International Journal for Numerical and Analytical Methods in Geomechanics*, 24:893–927, 2000.

[20] H. Matsuoka and T. Nakai. Stress–deformation and strength characteristics of soil under three different principal stresses. In *Proc. Japanese Soc. of Civil Engineers*, volume 232, pages 59–70, 1974.

[21] D. Mašín. A hypoplastic constitutive model for clays. *International Journal for Numerical and Analytical Methods in Geomechanics*, 29(4):311–336, 2005.

[22] D. Mašín. A hypoplastic constitutive model for clays with meta-stable structure. *Canadian Geotechnical Journal*, 44(3):363–375, 2007.

[23] D. Mašín. 3D modelling of a NATM tunnel in high K_0 clay using two different constitutive models. *Journal of Geotechnical and Geoenvironmental Engineering ASCE*, 135(9):1326–1335, 2009.

[24] D. Mašín. Comparison of predictive capabilities of selected elasto-plastic and hypoplastic models for structured clays. *Soils and Foundations*, 49(3):381–390, 2009.

[25] D. Mašín. Predicting the dependency of a degree of saturation on void ratio and suction using effective stress principle for unsaturated soils. *International Journal for Numerical and Analytical Methods in Geomechanics (in print)*, 2009.

[26] D. Mašín, V. Herbstová, and J. Boháč. Properties of double porosity clayfills and suitable constitutive models. In *Proc. 16th Int. Conference ICSMGE*, volume 2, pages 827–830. Osaka, Japan, 2005.

[27] D. Mašín and I. Herle. Numerical analyses of a tunnel in London clay using different constitutive models. In *In Proc. 5th Int. Symposium TC28 Geotechnical Aspects of Underground Construction in Soft Ground*, pages 595–600. Amsterdam, The Netherlands, 2005.

[28] D. Mašín and I. Herle. State boundary surface of a hypoplastic model for clays. *Computers and Geotechnics*, 32(6):400–410, 2005.

[29] D. Mašín and I. Herle. Improvement of a hypoplastic model to predict clay behaviour under undrained conditions. *Acta Geotechnica*, 2(4):261–268, 2007.

[30] D. Mašín and N. Khalili. A hypoplastic model for mechanical response of unsaturated soils. *International Journal for Numerical and Analytical Methods in Geomechanics*, 32(15):1903–1926, 2008.

[31] D. Mašín, C. Tamagnini, G. Viggiani, and D. Costanzo. Directional response of a reconstituted fine grained soil. Part II: performance of different constitutive models. *International Journal for Numerical and Analytical Methods in Geomechanics*, 30(13):1303–1336, 2006.

[32] J. Najser, D. Mašín, and J. Boháč. Numerical modelling of lumpy clay landfill. *International Journal for Numerical and Analytical Methods in Geomechanics (submitted)*, 2010.

[33] A. Niemunis. A visco-plastic model for clay and its FE implementation. In E. Dembicki, W. Cichy, and L. Balachowski, editors, *Recent results in mechanics of soils and rocks.*, pages 151–162. TU Gdańsk, 1996.

[34] A. Niemunis. *Extended hypoplastic models for soils.* Habilitation thesis, Ruhr-University, Bochum, 2002.

[35] A. Niemunis, C. E. Grandas Tavera, and L. F. Prada Sarmiento. Anisotropic visco-hypoplasticity. *Acta Geotechnica (in print)*, 2009.

[36] A. Niemunis and I. Herle. Hypoplastic model for cohesionless soils with elastic strain range. *Mechanics of Cohesive-Frictional Materials*, 2:279–299, 1997.

[37] E. P. Poeter and M. C. Hill. Documentation of UCODE, a computer code for universal inverse modelling. Technical report, US Geological Survey Water Resources Investigations Report 98-4080, 1998.

[38] K. H. Roscoe and J. B. Burland. On the generalised stress-strain behaviour of wet clay. In J. Heyman and F. A. Leckie, editors, *Engineering Plasticity*, pages 535–609. Cambridge: Cambridge Univesrity Press, 1968.

[39] S. E. Stallebrass and R. N. Taylor. Prediction of ground movements in overconsolidated clay. *Géotechnique*, 47(2):235–253, 1997.

[40] R. Suchomel and D. Mašín. Comparison of different probabilistic methods for predicting stability of a slope in spatially variable c-phi soil. *Computers and Geotechnics*, 37:132–140, 2010.

[41] D. A. Sun, D. Sheng, and Y. F. Xu. Collapse behaviour of unsaturated compacted soil with different initial densities. *Canadian Geotechnical Journal*, 44(6):673–686, 2007.

[42] T. Svoboda and D. Mašín. Impact of a constitutive model on inverse analysis of a NATM tunnel in stiff clays. In V. K. Kajnlia, T. Ramamurthy, P. P. Wahi, and A. C. Gupta, editors, *Proc. ITA-AITES World Tunnel Congress, Agra, India*, volume 2, pages 627–636. Springer, Berlin, 2008.

[43] T. Svoboda and D. Mašín. Evaluation of the convergence-confinement method on the basis of 3D analyses of several shallow NATM tunnels in clays. *Under review*, 2009.

[44] T. Svoboda and D. Mašín. Optimisation of parameters for simulating a natm tunnel in stiff clays based on a 3d model of exploratory adit. In G. Meschke, G. Beer, J. Eberhardsteiner, D. Hartmann, and M. Thewes, editors, *Proc. 2^{nd} International Conference on Computational Methods in Tunnelling EURO:TUN 2009*, volume 1, pages 249–256, 2009.

[45] J. Trhlíková, D. Mašín, and J. Boháč. Modelling of the small strain behaviour of cemented soils. *Géotechnique, submitted*.

[46] G. Viggiani and J. H. Atkinson. Stiffness of fine–grained soil at very small strains. *Géotechnique*, 45(2):245–265, 1995.

[47] P. A. von Wolffersdorff. A hypoplastic relation for granular materials with a predefined limit state surface. *Mechanics of Cohesive-Frictional Materials*, 1:251–271, 1996.

Appendix - selected key publications

The following key publications form Appendix part of the Habilitation thesis:

- D. Mašín. A hypoplastic constitutive model for clays. *International Journal for Numerical and Analytical Methods in Geomechanics*, 29(4):311–336, 2005.
- D. Mašín and I. Herle. State boundary surface of a hypoplastic model for clays. *Computers and Geotechnics*, 32(6):400–410, 2005.
- G. Gudehus and D. Mašín. Graphical representation of constitutive equations. *Géotechnique*, 52(2):147–151, 2009.
- D. Mašín. A hypoplastic constitutive model for clays with meta-stable structure. *Canadian Geotechnical Journal*, 44(3):363–375, 2007.
- D. Mašín and N. Khalili. A hypoplastic model for mechanical response of unsaturated soils. *International Journal for Numerical and Analytical Methods in Geomechanics*, 32(15):1903–1926, 2008.
- D. Mašín. Predicting the dependency of a degree of saturation on void ratio and suction using effective stress principle for unsaturated soils. *International Journal for Numerical and Analytical Methods in Geomechanics (in print)*, 2009.
- G. Gudehus, A. Amorosi, A. Gens, I. Herle, D. Kolymbas, D. Mašín, D. Muir Wood, R. Nova, A. Niemunis, M. Pastor, C. Tamagnini, and G. Viggiani. The soilmodels.info project. *International Journal for Numerical and Analytical Methods in Geomechanics*, 32(12):1571–1572, 2008.
- D. Mašín. 3D modelling of a NATM tunnel in high K_0 clay using two different constitutive models. *Journal of Geotechnical and Geoenvironmental Engineering ASCE*, 135(9):1326–1335, 2009.